Fermi National Accelerator Laboratory

FERMILAB-Pub-92/244-E

Measurement of the Proton Electromagnetic Form Factors in the Time-Like Region at 8.9 to 13.0 GeV^2

T.A. Armstrong *et al.*

(The E760 Collaboration)

Fermi National Accelerator Laboratory, Batavia, Illinois 60510

September 1992

Submitted to *Physical Review Letters*

Operated by Universities Research Association Inc. under Contract No. DE-AC02-76CHO3000 with the United States Department of Energy

Disclaimer

FERMILAB-Pub-92/244-E

Measurement of the Proton Electromagnetic Form Factors in the Time-Like Region at 8.9 to 13.0 GeV^2

T.A. Armstrong[6], D. Bettoni[2], V. Bharadwaj[1], C. Biino[7], G. Borreani[2], D. Broemmelsiek[4], A. Buzzo[3], R. Calabrese[2], A. Ceccucci[7], R. Cester[7], M.D. Church[1], P. Dalpiaz[2], P.F. Dalpiaz[2], R. Dibenedetto[7], D. Dimitroyannis[5], M.G. Fabbri[2], J.E. Fast[4], A. Gianoli[2], C.M. Ginsburg[5], K.E. Gollwitzer[4], A.A. Hahn[1], M.A. Hasan[6], S.Y. Hsueh[1], R.A. Lewis[6], E. Luppi[2], M. Macrí[3], A. Majewska[6], M.A. Mandelkern[4], F. Marchetto[7], M. Marinelli[3], J.L. Marques[4], W. Marsh[1], M. Martini[2], M. Masuzawa[5], E. Menichetti[7], A. Migliori[7], R. Mussa[7], S. Palestini[7], M. Pallavicini[3], N. Pastrone[7], C. Patrignani[3], J. Peoples, Jr.[1], L. Pesando[7], F. Petrucci[2], M.G. Pia[3], S. Pordes[1], P.A. Rapidis[1], R.E. Ray[5*], J.D. Reid[6], G. Rinaudo[7], B. Roccuzzo[7], J.L. Rosen[5], A. Santroni[3], M. Sarmiento[5], M. Savrié[2], A. Scalisi[3], J. Schultz[4], K.K. Seth[5], A. Smith[4], G.A. Smith[6], M. Sozzi[6], S. Trokenheim[5], M.F. Weber[4], S.J. Werkema[1], Y. Zhang[6], J.L. Zhao[5], G. Zioulas[4].

(E-760 Collaboration)

[1] *Fermi National Accelerator Laboratory, Batavia, Illinois 60510*
[2] *I.N.F.N. and University of Ferrara, I-44100 Ferrara, Italy*
[3] *I.N.F.N. and University of Genoa, I-16146 Genoa, Italy*
[4] *University of California at Irvine, California 92717*
[5] *Northwestern University, Evanston, Illinois 60208*
[6] *Pennsylvania State University, University Park, Pennsylvania 16802*
[7] *I.N.F.N. and University of Turin, I-10125 Turin, Italy*

Cross sections for the reaction $p\bar{p} \to e^+e^-$ have been measured at $s = 8.9, 12.4,$ and 13.0 GeV^2. The cross sections have been analyzed to obtain the proton electromagnetic form factors in the time-like region.

PACS numbers: 13.40.Fn, 12.38.Qk, 14.20.Dh

The understanding of nucleon structure is one of the central problems of hadronic physics. Measurements of the electric and magnetic form factors, G_E and G_M, as functions of the four-momentum transfer q^2 provide experimental information relating to the nucleon structure. A large body of precise data obtained primarily from elastic scattering of electrons by protons and deuterons now exists for these form factors, with the form factors of the proton known up to $q^2 = 31$ $(\mathrm{GeV/c})^2$[1]. However these data are primarily for space-like momentum transfers ($q^2 \geq 0$). Precise results for G_M in the time-like region ($s = -q^2c^2 > 0$) exist only for a small interval near threshold, $4m_p^2c^4 \leq s \leq 4.2$ GeV^2. These data were recently obtained at the LEAR facility at CERN from the reaction $p\bar{p} \rightarrow e^+e^-$ [2]. For larger momentum transfers only upper limits have been established by earlier $e^+e^- \rightarrow p\bar{p}$ and $p\bar{p} \rightarrow e^+e^-$ experiments[3]. Perturbative QCD predicts[4] that for large momentum transfers $q^4|G_M|/\mu_p$ should be nearly proportional to the square of the running coupling constant for strong interactions, $\alpha_s^2(q^2)$. Recent data[1] for large space-like momentum transfers are in remarkable agreement with this prediction for q^2 as small as 5 $(\mathrm{GeV/c})^2$. It is of great interest to find out if a similar behavior holds for time-like momentum transfers.

In this letter we present the results of our measurements of the cross section for the reaction

$$p\bar{p} \rightarrow e^+e^- \tag{1}$$

at $\sqrt{s}$ = 3.0 GeV, 3.5 GeV, and 3.6 GeV. These measurements were made as a part of Fermilab experiment E760, which is dedicated to the study of charmonium by resonant formation in $p\bar{p}$ annihilations[5]. The differential cross section for process (1) can be expressed in terms of the proton magnetic and electric form factors as[6]:

$$\frac{d\sigma}{d(cos\theta^*)} = \frac{\pi\alpha^2(\hbar c)^2}{8\ E\ P}$$

$$\times\left[|G_M|^2(1+cos^2\theta^*) + \frac{4m_p^2}{s}|G_E|^2 sin^2\theta^*\right] \tag{2}$$

where E and P are the center of mass energy and momentum of the antiproton, and θ^* is the angle between the e^- and the $\bar{p}$ in the center of mass system.

Experiment E760 has been carried out at the antiproton accumulator of the Fermilab Antiproton Source. The circulating beam of stochastically cooled antiprotons (up to $4\times10^{11}\bar{p}$) intersects an internal hydrogen gas jet target to provide instantaneous luminosities up to $9 \times 10^{30}\mathrm{cm}^{-2}\mathrm{s}^{-1}$.

The detector (Fig. 1) is a non-magnetic spectrometer with cylindrical symmetry about the beam axis[7], optimized for the detection of electromagnetic final states. The central calorimeter covers the full azimuth and $11° < \theta < 70°$, and consists of an assembly of 1280 lead glass detectors, each pointing to the beam-jet interaction region. The planar forward calorimeter covers $2° < \theta < 11°$, and consists of 144 lead-scintillator sandwich detectors. A threshold gas Čerenkov counter, with two-fold

polar and eight-fold azimuthal segmentation, allows discrimination between electrons and charged hadrons. A coincidence between the appropriate azimuthal elements of two scintillator hodoscopes (H1 and H2) with the corresponding cells of the Čerenkov counter, and at least two large energy deposits in the central calorimeter separated by $\Delta\phi > 90°$, define the fast trigger for *two electron* events. The efficiency of this trigger has been measured at both J/ψ and ψ' formation energies as $\epsilon_{trig} = 0.92 \pm 0.02$[5]. Charged particle tracking information is provided by three inner elements, a cylindrical straw chamber, a radial projection chamber (RPC), and a multiwire proportional chamber, as well as an outer element consisting of two layers of limited streamer tubes. The luminosity is determined by detecting recoil protons in a solid-state detector mounted at $\theta = 86.5°$, and normalizing the yield to the known $p\bar{p}$ elastic scattering cross sections.

The off-line analysis of the data is based on the identification of two electron tracks collinear in the center of mass, with an invariant mass $m_{e^+e^-}$ compatible with the center of mass energy ($\sqrt{s}$) of the $p\bar{p}$ system. The fiducial range of polar angle in which the electrons are accepted is $15° < \theta < 60°$. A preliminary selection requires the two highest energy showers in the central calorimeter to be associated with the electron track candidates. The electron identification is based on the pulse height information from the hodoscope H2 and the Čerenkov counter, dE/dx information from the RPC, and the transverse shape of the energy deposition in the central calorimeter[5]. The e^+e^- invariant mass distribution at this stage of the selection is shown in Figs. 2 (a),(b), and (c), respectively for $\sqrt{s} = 3.0$ GeV, 3.5 GeV, and 3.6 GeV. A feature common to the three distributions is the presence of a low invariant mass background, which we attribute to residual Dalitz pairs or photon conversions from the vast π^0 component of the $p\bar{p}$ annihilation. In addition, Figs. 2 (b) and (c) show a prominent signal corresponding to the inclusive production of J/ψ and its subsequent decay, $J/\psi \to e^+e^-$[8]. Both the background and the J/ψ signal disappear when we require only two showers in the electromagnetic calorimeter and impose the requirements of two body kinematics on the electron directions. From a study of a background-free sample of $p\bar{p} \to J/\psi \to e^+e^-$ events, we determine our angular resolution and apply $\pm 2.5\sigma$ cuts on the azimuthal and polar collinearity: specifically we require $178.3° < \phi_{ee} < 181.7°$ and $177° < \theta^*_{ee} < 183°$ where ϕ_{ee} is the azimuthal angle between the two electrons, and θ^*_{ee} is the sum of the center of mass polar angles of the two electrons with respect to the antiproton direction. The events remaining after these cuts are shown as the shaded area in Fig. 2 and are seen to cluster around the corresponding center of mass energy with a spread compatible, to within ± 2 standard deviations, with the experimental mass resolution. Notice that no cut on the e^+e^- invariant mass has been necessary to obtain a very low background sample of events belonging to reaction (1). The efficiency of the above event selection, determined by using the e^+e^- events from the J/ψ and ψ' data samples, is found to be $\epsilon_{sel} = 0.79 \pm 0.03$. Thus the overall efficiency is $\epsilon = \epsilon_{trig} \cdot \epsilon_{sel} = 0.73 \pm 0.03$. Fig. 3 shows the θ^*_{ee} distribution for events with only two clusters in the central calorimeter

if, alternatively, we cut on the azimuthal opening angle ϕ_{ee} and on the e^+e^- invariant mass. This sample includes all events found with the previous selection.

Two-pion final states are the main source of background for reaction (1). The cross section, $\sigma(p\bar{p} \to \pi^+\pi^-)$ is known to be $\leq 10\mu$b for $3.0 \leq \sqrt{s} \leq 3.6$ GeV[9]. The pion contamination is measured from a sample of resolved $p\bar{p} \to \pi^+\pi^-$ events that were collected with a dedicated hadron trigger. From these we measure a probability of 2×10^{-3} for a pion to produce a shower in the central calorimeter which simulates an electromagnetic shower with an energy compatible with the two-body kinematics of the e^+e^- final state, and a 1.2×10^{-2} probability for a pion to produce a Čerenkov signal that would pass the selection criteria used to define an electron. The combined calorimeter and Čerenkov rejection for $\pi^+\pi^-$ events is thus 1.6×10^9. This leads to an estimated background cross section ≤ 0.01 pb, which is negligible when compared to the measured cross section.

The $p\bar{p} \to \pi^0\pi^0$ annihilation is also a source of possible background, when each of the two π^0's either undergoes a Dalitz decay or has one of the two decay photons converted in the 0.2 mm stainless steel wall of the beam pipe. This background has been estimated from data collected in the same experiment with an all neutral trigger designed to detect $p\bar{p} \to \gamma\gamma$ events. These data provide the cross section for neutral events with just two clusters in the central calorimeter satisfying the kinematic constraints used to select reaction (1). The measurement gives a cross section of 800 pb at $\sqrt{s} = 3.0$ GeV and 100 pb at $\sqrt{s} = 3.5$ GeV. Taking into account the conversion probability (2%) per photon and the probability for both pairs to be misidentified as single electrons(5%) we estimate a background cross section from photon conversions to be ≤ 0.016 pb at $\sqrt{s} \approx 3.0$ GeV and ≤ 0.002 pb at $\sqrt{s} \approx 3.5$ GeV, which is also negligible. Similar contributions come from one or both π^0's decaying into a Dalitz pair. In conclusion, we estimate the total background from all sources to be less than 0.3 events among the 29 events observed.

The e^+e^- events from the decay in the tails of the J/ψ and ψ' resonances constitute a possible background for the form factor events of reaction (1). This contribution has been calculated to be negligible.

We recall that the fiducial range has been restricted to $15° < \theta < 60°$; this corresponds to different acceptance ranges for $cos\theta^*$ at different energy values. For a given integrated luminosity $\mathcal{L}$, and overall efficiency ϵ, the number of events is:

$$N = \epsilon \, \mathcal{L} \, \sigma_{corr}, \tag{3}$$

with

$$\sigma_{corr} = \int_{-cos\theta^*_{max}}^{cos\theta^*_{max}} d(cos\theta^*) \frac{d\sigma}{d(cos\theta^*)}$$

$$= \frac{\pi\alpha^2(\hbar c)^2}{8 \, E \, P} \Big[A|G_M|^2 + B|G_E|^2 \Big] \tag{4}$$

where

$$A = 2\int_0^{cos\theta^*_{max}} d(cos\theta^*)(1 + cos^2\theta^*) \tag{5}$$

and

$$B = 2\int_0^{cos\theta^*_{max}} d(cos\theta^*)\frac{4m_p^2}{s}sin^2\theta^* \tag{6}$$

In Table I we present the values of $s = -q^2$, $cos\theta^*_{max}$, A, B, and σ_{corr}. The cross sections σ_{corr} are obtained from Eq. (4). Due to the limited statistics and angular coverage we cannot derive G_E and G_M separately. The values of $|G_M|$ are deduced from Eq. (5) under the two assumptions: (a) $|G_E| = |G_M|$, and (b) neglecting the term containing G_E and are reported in table I. It is to be noted that the values of $|G_M|$ determined under the two approximations differ by less than 15%. The values of the proton magnetic form factor, under assumption (a), are shown in fig. 4 (a).

In Fig. 4 (b) we plot the same set of values for $|G_M|$ in the form of $q^4|G_M|/\mu_p$ versus $-q^2$ ($\mu_p = 2.79$), along with the earlier results from the literature[2]. The curve corresponds to $G_M(q^2) \propto q^{-4}\alpha_s^2(q^2)$, where $\alpha_s(q^2)$ is proportional to $1/ln(q^2/\Lambda^2)$, with $\Lambda = 0.2$ GeV. The dependence on q^2 is consistent with what was found for comparable space-like momentum transfers[1], however the numerical values of $|G_M|$ in the time-like region are nearly twice as large as those in the corresponding space-like region.

The fit presented in Fig. 4 (b) leads to the estimate that $|G_M(q^2 = M^2_{J/\psi})| = 0.026 \pm 0.002$ and $|G_M(q^2 = M^2_{\psi'})| = 0.012 \pm 0.001$. By integrating Eq. (2) and then applying the principle of detailed balance, we obtain the total cross sections:

$$\text{at } M_{J/\psi},\ \ \sigma_T(e^+e^- \to \gamma^* \to p\overline{p}) = (5.9 \pm 0.9)\text{ pb} \tag{7}$$

$$\text{at } M_{\psi'},\ \ \sigma_T(e^+e^- \to \gamma^* \to p\overline{p}) = (0.83 \pm 0.13)\text{ pb} \tag{8}$$

The cross section $\sigma_T(e^+e^- \to \gamma^* \to hadrons)$ in the continuum is given by $[4\pi\alpha^2(\hbar c)^2/3] \times R/s$, where the ratio $R = \sigma(e^+e^- \to hadrons)/\sigma(e^+e^- \to \mu^+\mu^-)$ has the measured value of 2.5 ± 0.2 in this mass region[10][11]. Thus the branching fractions

$$f(\gamma*) \equiv \frac{\sigma_T(e^+e^- \to \gamma^* \to p\overline{p})}{\sigma_T(e^+e^- \to \gamma^* \to hadrons)} \tag{9}$$

are $(2.6\pm0.5)\times10^{-4}$ at the J/ψ, and $(0.52\pm0.09)\times10^{-4}$ at the ψ'. The corresponding branching fractions for gluonic decays of the J/ψ and the ψ'

$$f(ggg) \equiv \frac{\Gamma(R_c \to ggg \to p\overline{p})}{\Gamma(R_c \to ggg \to hadrons)} \tag{10}$$

are estimated to be $(31 \pm 2) \times 10^{-4}$ and $(12 \pm 4) \times 10^{-4}$ for the J/ψ and ψ' respectively. A comparison of these branching fractions leads us to the purely experimental result that the hadronization via gluons favours the $p\bar{p}$ channel by approximately an order of magnitude as compared to hadronization via a photon.

We gratefully acknowledge the technical support from our collaborating institutions and the outstanding contribution of the Fermilab Accelerator Division. This work was supported in part by the U.S. Department of Energy, the U.S. National Science Foundation and the Italian Istituto Nazionale di Fisica Nucleare.

REFERENCES

* Now at Fermi National Accelerator Laboratory, Batavia, Illinois 60510.

[1] R.G. Arnold *et al.*, Phys. Rev. Lett. **57**, 174 (1986); P.E. Bosted *et al., ibid.* **68**, 3841 (1992).

[2] G. Bardin *et al.*, Phys. Lett. B **255**, 149 (1991); **257**, 514 (1991). References to the original sources of the earlier data shown in Fig.4 may also be found there.

[3] C. Baglin *et al.*, Phys. Lett. B **163**, 400 (1985); D. L. Hartill *et al.*, Phys. Rev. **184**, 1415 (1969); M. Conversi *et al.*, Nuovo Cimento **40**, 690 (1965).

[4] G.P. Lepage and S.J. Brodsky, Phys. Rev. Lett. **43**, 545 (1979); Phys. Rev. D **22**, 2157 (1980).

[5] T.A. Armstrong *et al.*, Report No. FERMILAB-Pub-92/245-E, September 1992, submitted to Phys. Rev. D.; Nucl. Phys. B **373**, 35 (1992).

[6] A. Zichichi, S.M. Berman, N. Cabibbo, and R. Gatto, Nuovo Cimento **24**, 170 (1962).

[7] L. Bartoszek *et al.*, Nucl. Instrum. Methods **A301**, 47 (1991); C. Biino *et al.*, *ibid.* **A271**, 417 (1988); **A317**, 135 (1992); R. Calabrese *et al., ibid.* **A277**, 116 (1989); M.A. Hasan *et al., ibid.* **A295**, 73 (1990); R. Ray *et al., ibid.* **A307**, 254 (1991); C. Biino *et al.*, IEEE Trans. Nucl. Sci. **36**, 98 (1989); R. Calabrese *et al.*, *ibid.* **36**, 54 (1989).

[8] T.A. Armstrong *et al.*, Report No. FERMILAB-Pub-92/186-E, July 1992, submitted to Phys. Rev. Lett.

[9] V. Flaminio *et al., Compilation of Cross Sections - III: p and $\overline{p}$ Induced Reactions*, Report No. CERN-HERA 84-01 (1984).

[10] Particle Data Group, "Review of Particle Properties", Phys. Rev. D **45**, S1 (1992).

[11] P.A. Rapidis *et al.*, Phys. Rev. Lett. **39**, 526 (1977); P.A. Rapidis, thesis, SLAC-Report 220(1979); J.L. Siegrist *et al.*, Phys. Rev. D **26**, 969 (1982).

FIGURES

FIG. 1. Layout of the E760 detector and the gas jet.

FIG. 2. Distribution of the e^+e^- invariant mass for events collected at: (a) s = 8.9 GeV^2, (b) s = 12.4 GeV^2, and (c) s = 13.0 GeV^2. The open histograms are for events passing the preliminary event selection. The shaded histograms are for events which survive the final collinearity cut.

FIG. 3. θ^*_{ee} for e^+e^- coplanar pairs with an invariant mass compatible with the c.m. energy of the interaction for events with only two clusters in the calorimeter at : (a) s = 8.9 GeV^2, (b) s = 12.4 GeV^2, and (c) s = 13.0 GeV^2.

FIG. 4. Variation of $|G_M|$ and $q^4|G_M|/\mu_p$ versus $-q^2$. The crosses are from the present experiment. For the sources of the other data shown see Ref. [2]. (a) $|G_M|$ versus $-q^2$. (b) $q^4|G_M|/\mu_p$ versus $-q^2$; the dashed curve shows the perturbative QCD fit to the data for $q^2 \geq 5$ (GeV/c)^2 described in the text.

TABLES

TABLE I. Summary of results for the magnetic form factor of the proton.

s (GeV^2)	$\mathcal{L}$ (pb^{-1})	$N_{e^+e^-}$	σ_{corr} (pb)	$\lvert cos\theta^*_{max}\rvert$	A	B	$\lvert G_M\rvert$ (a)	$\lvert G_M\rvert$ (b)
8.9	2.8 ± 0.1	14	$6.8^{+2.3}_{-1.8}$	0.45	0.96	0.33	$0.033^{+.006}_{-.004}$	$0.039^{+.007}_{-.005}$
12.4	17.7 ± 0.9	11	$0.85^{+.34}_{-.25}$	0.60	1.34	0.30	$0.013^{+.003}_{-.002}$	$0.014^{+.003}_{-.002}$
13.0	6.0 ± 0.3	4	$0.91^{+.72}_{-.44}$	0.62	1.40	0.29	$0.013^{+.005}_{-.003}$	$0.015^{+.006}_{-.004}$

The G_M values in column (a) are obtained with the assumption $|G_E| = |G_M|$. Those in column (b) are obtained by neglecting the contribution of the term containing G_E.

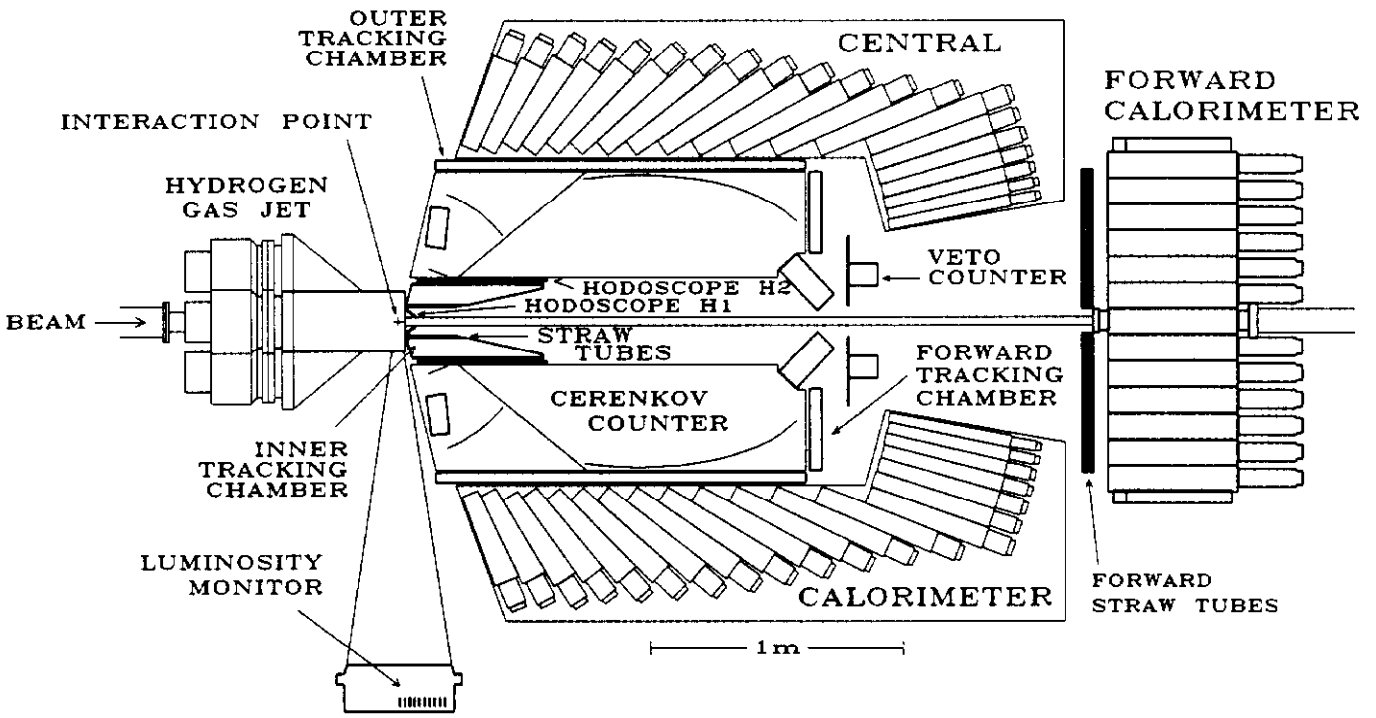

FIG. 1. Layout of the E760 detector and the gas jet.

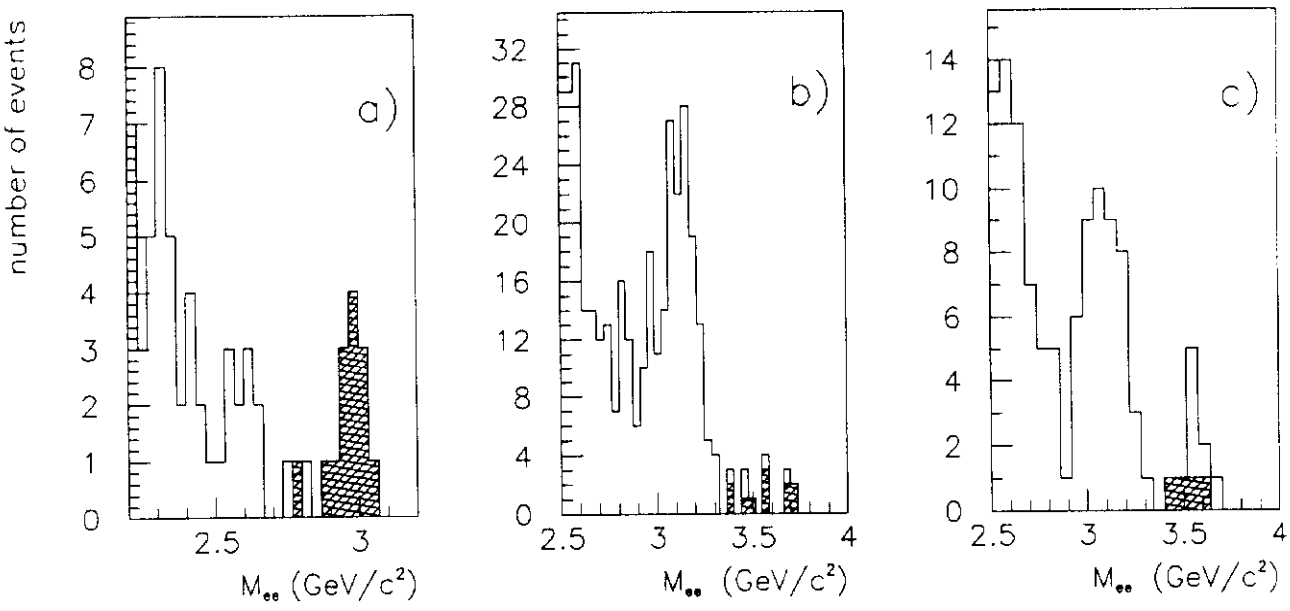

FIG. 2. Distribution of the e^+e^- invariant mass for events collected at: (a) s = 8.9 GeV^2, (b) s = 12.4 GeV^2, and (c) s = 13.0 GeV^2. The open histograms are for events passing the preliminary event selection. The shaded histograms are for events which survive the final collinearity cut.

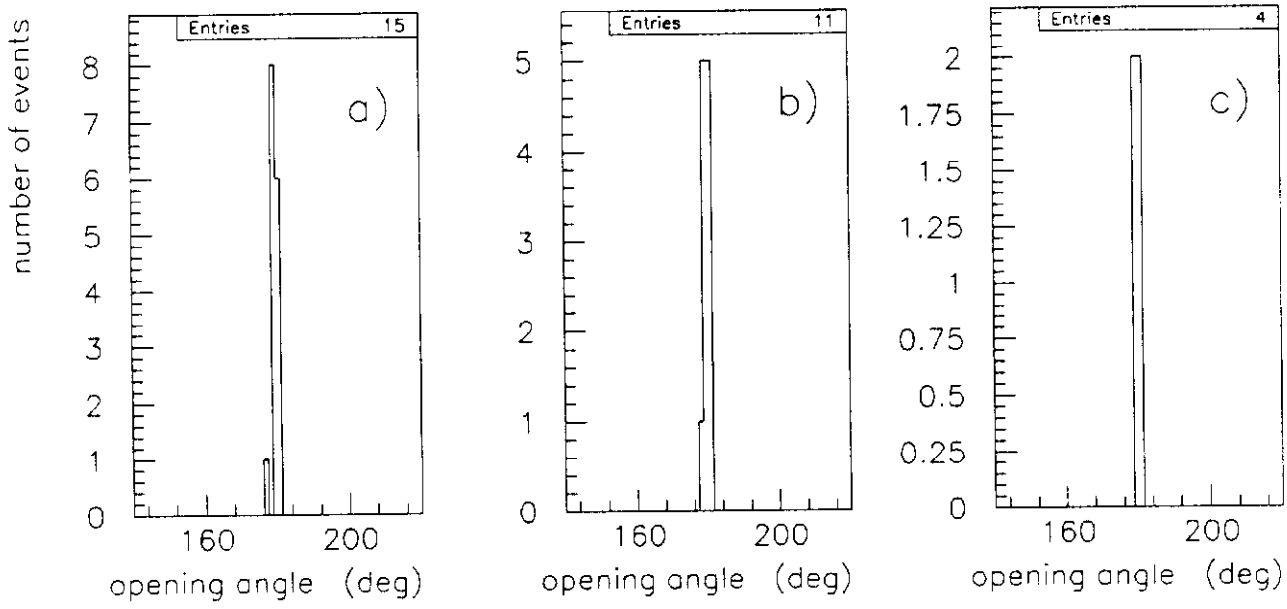

FIG. 3. θ^*_{ee} for e^+e^- coplanar pairs with an invariant mass compatible with the c.m. energy of the interaction for events with only two clusters in the calorimeter at : (a) s = 8.9 GeV^2, (b) s = 12.4 GeV^2, and (c) s = 13.0 GeV^2.

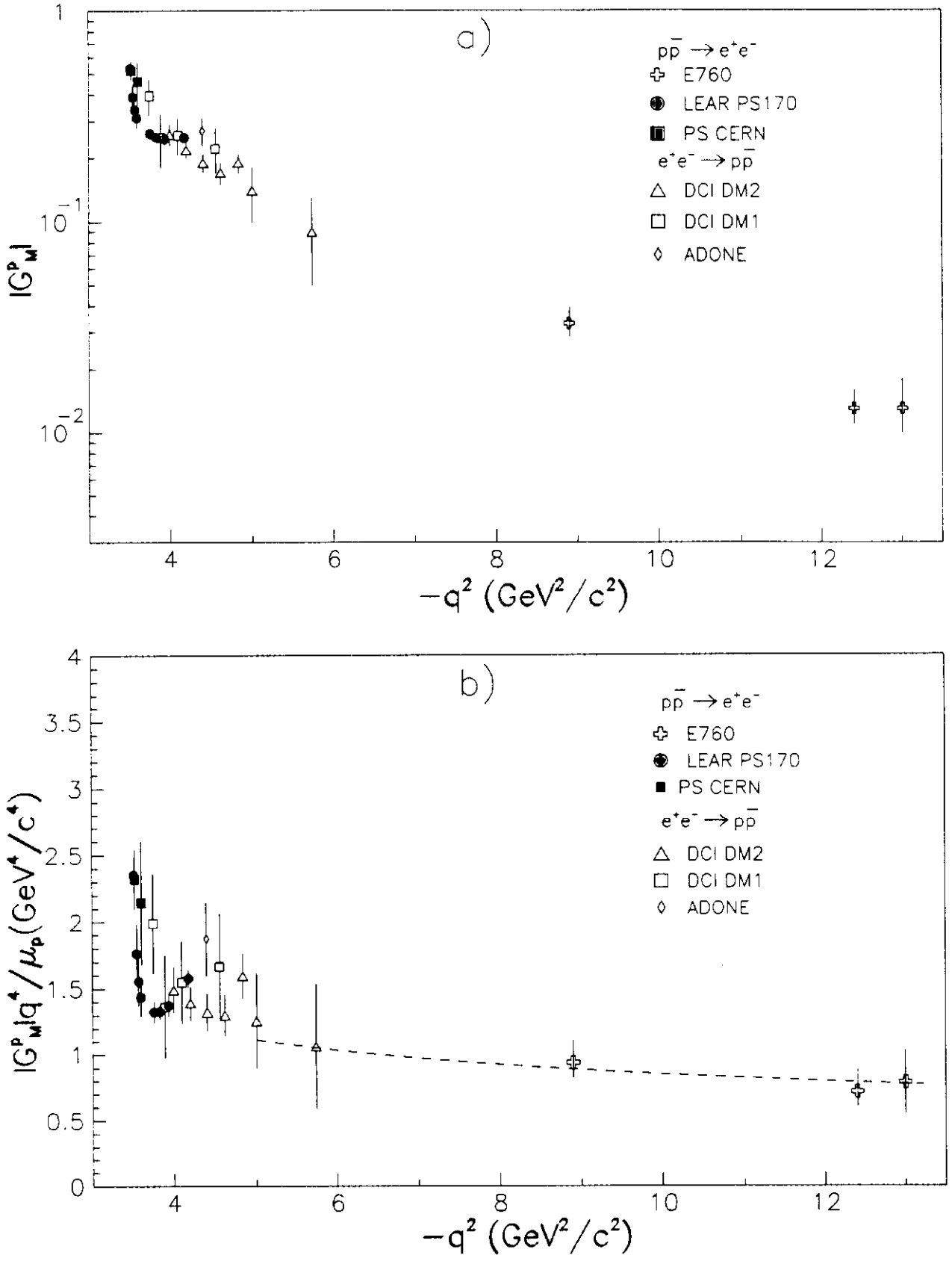

FIG. 4. Variation of $|G_M|$ and $q^4|G_M|/\mu_p$ versus $-q^2$. The crosses are from the present experiment. For the sources of the other data shown see Ref. [2]. (a) $|G_M|$ versus $-q^2$. (b) $q^4|G_M|/\mu_p$ versus $-q^2$; the dashed curve shows the perturbative QCD fit to the data for $q^2 \geq 5$ (GeV/c)^2 described in the text.